

Polymer Films on Electrodes

VII. Electrochemical Behavior at Polypyrrole-Coated Platinum and Tantalum Electrodes

Randy A. Bull, Fu-Ren F. Fan, and Allen J. Bard*

Department of Chemistry, The University of Texas at Austin, Austin, Texas 78712

ABSTRACT

Polypyrrole films were deposited on platinum and tantalum and used as electrodes. The results indicate that these films are porous to solvent and electrolyte ions, and this porosity is responsible for the apparent reversible electrochemical behavior previously observed with many redox couples at polypyrrole on Pt. These electrochemically conducting films do exhibit electron transfer reactions with solution species, although less reversibly than at naked or film-covered Pt. The films are unstable to oxidative conditions such as potentials $> 0.6V$ vs. SCE or the presence of halogens.

Polymer coatings on electrode surfaces have been employed to incorporate electrocatalysts (1), to stabilize the substrate from attack (2), and as analytical probes and reference electrodes (3). An especially interesting class of polymers are the electronically conductive materials, such as polypyrrole (PP), which can be prepared as films on metal substrates by electrochemical polymerization. The preparation and properties of such films, first reported in 1968 (4), have been investigated by Diaz and co-workers (5). Recently PP coatings have been employed to protect semiconductor electrodes from photocorrosion (6, 7).

Although the solid-state properties and some of the redox chemistry of PP films on Pt have been investigated (5), there have been few studies on the mechanisms of electrochemical reactions of solution species at PP. For an electronically conductive polymer like PP, several mechanisms are possible. The film itself can behave as the electrode material; in this case, the electrochemical properties should be relatively independent of the substrate, and any electrocatalysis (e.g., for hydrogen evolution) should be characteristic of PP. However, transport of electroactive species via pores or channels in the film with reaction at the substrate is also possible (8). Another important aspect of PP films, in connection with their use as stabilizing layers on metals or semiconductors, is their stability to strong oxidants such as Cl_2 or Br_2 .

We report here on the properties of PP as an electrode material and its characterization by voltammetric and impedance measurements. To test for substrate effects, we compared platinum and tantalum as backing materials for the PP films. Platinum represents an electrochemically active substrate while tantalum is readily passivated (9) so that any activity observed with Ta/PP should not be attributable to diffusion of solution species through the polymer film. Impedance measurements, which have been applied extensively to the study of the electrochemical responses of porous electrodes (10), provide evidence that penetration of the electrolyte solution into the polymer matrix occurs.

Experimental

Electrode preparation.—Ta disk electrodes were made from 0.127 mm Ta foil (Alfa) cemented in glass tubing with Devcon 5 min epoxy and sealed with Dow Corning silicone rubber sealant. Contact was made to the back of the foil with conductive silver paint which was insulated from the solution with epoxy cement. These electrodes were polished with successively finer grades of carborundum and finally with 0.3 and 0.05 μm alumina on felt. The Pt disk electrodes were sealed in glass and polished in a similar way. Before each new set of experiments the electrodes were repolished with 0.05 μm alumina and buffed with felt.

* Electrochemical Society Active Member.

Key words: cyclic voltammetry, impedance measurements, electrochemistry of solution redox species.

Polypyrrole deposition.—PP films were deposited electrochemically (5d) onto Pt and Ta electrodes from solutions containing 0.2M tetra-n-butylammonium fluoroborate $TBABF_4 \cdot CH_3CN$ (Spectrograde) and 1M PP (distilled from CaH_2) by stepping the potential to $+0.95V$ vs. an Ag wire reference electrode in a stirred solution under N_2 . Film deposition was monitored by measuring the charge passed and film thicknesses were estimated assuming 24 mC/cm^2 charge yielded 0.1 μm film (5c). Measurements on dry films with a Sloan Dektak Profilometer yielded thicknesses within $\pm 20\%$ of these estimates.

Electrochemical measurements.—A Princeton Applied Research Corporation (PAR) Model 173 potentiostat, PAR Model 175 universal programmer, and PAR Model 179 digital coulometer were employed. The reference electrode in all voltammetric measurements was an aqueous saturated calomel electrode (SCE) and the counterelectrode was a Pt wire.

The impedance measurements were performed according to the procedures reported previously (11). A gold foil (~ 50 cm^2) was used as the counterelectrode. The capacitance was measured as the 90° quadrature signal from a lock-in amplifier (PAR Model HR-8). The measured capacitances were calibrated by replacing the electrochemical cell by a set of standard capacitors. The parallel resistance was measured as the in-phase signal. The measured resistances were calibrated by a set of standard resistors. All solutions were prepared from triply distilled water and were deoxygenated for at least 30 min with purified nitrogen before each experiment. During the experiments the solutions were kept under a nitrogen atmosphere.

Results

Polypyrrole deposition.—Films could be deposited from MeCN/ $TBABF_4$ with little difficulty on both Pt and polished Ta. The current-time responses during deposition differed with the two substrates. The current increased slightly with continued deposition on Pt by ~ 1 to 2 $\mu A/cm^2/sec$. For deposition onto Ta the increase was more than twice that initially, but once the film thicknesses became $> 0.8 \mu m$, the rate decreased to about that observed on Pt. The films adhered well to both Pt and Ta.

Cyclic voltammetry (CV) in background solutions.—CV scans for PP on both Pt and Ta in 0.2M $TBABF_4 \cdot MeCN$ showed very large background currents in the potential region where the film is not oxidized or reduced (0 to $+0.6V$ vs. SCE). The CV traces resembled pure capacitive currents (Fig. 1) in that for scan rates, v , of 10 to 50 mV/sec the currents, i_c , varied linearly with v , and upon scan reversal at any potential, the current immediately changed sign. The capacitances, measured from i_c/v , were of the order of mF/cm^2 (compared to the usual $\mu F/cm^2$ values for the bare

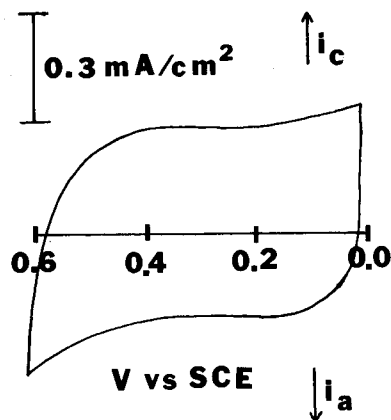


Fig. 1. Cyclic voltammogram for 0.15 μm PP on Ta in 0.2M TBABF₄-MeCN. $\nu = 100$ mV/sec.

electrodes). At faster scan rates ($\nu > 100$ mV/sec) and for thick films ($> 0.6 \mu\text{m}$), i_c varied linearly with $\nu^{1/2}$ (Table I). Similar behavior was observed with aqueous solutions (e.g., 0.1N H₂SO₄).

When the scan was extended beyond this region, the PP films (0.1–1.0 μm) on both Pt and Ta underwent oxidation and reduction reactions (0.2M TBABF₄-MeCN). A typical scan for Ta/PP is shown in Fig. 2. A broad reduction peak was observed at ~ -0.35 V vs. SCE after which the current decreased sharply due to the insulating nature of the film (5). The film oxidation following reduction occurred at ~ 0.0 V. The anodic peak current, i_{pa} , varied linearly with ν up to 50 mV/sec. The integrated area of this peak corresponded to a charge 8–11% of the charge passed on deposition and was about the same as that observed for PP films on Pt (5). For thicker films (0.6–1.0 μm), this integrated charge was 3% of the deposition charge. The charges passed in film oxidation and reduction were nearly equal.

The polymer films were stable to cycling between -1.0 and 0.6 V in MeCN. Extending the negative limit had little effect on the CV characteristics. After holding at a potential of -1.0 V, a subsequent anodic scan restored most of the current observed in the initial scans. However, when the film was taken to potentials $> +0.8$ V the current was smaller, at a given potential and ν , than that found before electrode oxidation. Maintaining a potential of $+1.0$ V for 30 sec resulted in a permanent decrease in current by 30–50%. However, there was no visible evidence of film deterioration following this treatment.

The reduction of the PP on Pt in 0.1N H₂SO₄ could not be observed because of the onset of proton reduction at ~ -0.3 V. On Ta, however, the film redox behavior was similar to that in MeCN, with both the reduction and oxidation peaks being broader and cen-

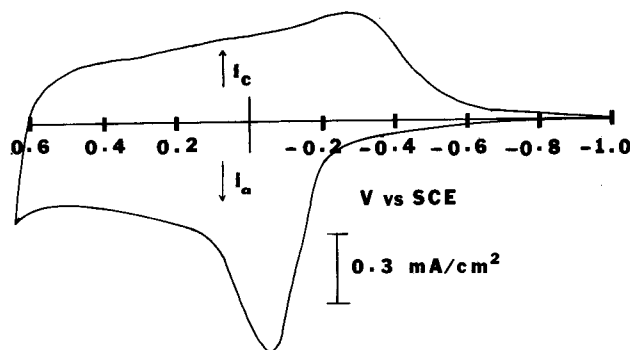


Fig. 2. Cyclic voltammogram for 0.15 μm PP on Ta in 0.2M TBABF₄-MeCN. $\nu = 100$ mV/sec.

tered at -0.35 and -0.05 V, respectively. The films on Ta were less stable to cycling in this potential region in 0.1N H₂SO₄, and both the large background currents and the peak currents decreased on continued cycling.

The facts that proton reduction occurs at Pt/PP and Ta/PP at very different potentials and that the hydrogen-evolution reaction on Pt/PP takes place at potentials close to that observed on bare Pt in the same medium are strong evidence for the penetration of the PP film by solution followed by redox reactions at the substrate.

When films on Pt and Ta were scanned to more positive potentials, a large anodic peak was observed at $\sim +1.0$ V. This disappeared after the first scan, and the peak currents decreased to $\sim 50\%$ of those observed before cycling through that peak. Successive scans to the onset of this wave resulted in a gradual decrease of film redox currents. This wave was not observed in MeCN.

The redox behavior of PP on Ta in 10.5M LiCl showed only a slight decrease in currents on continued cycling between -1.0 and $+0.6$ V. Reduction and oxidation peaks were observed at -0.3 and 0 V, respectively. Similar results were obtained for films on Pt. Scanning to potentials $> +0.8$ V resulted in a decrease in currents in the intermediate region. Stability in the presence of halogens is discussed below.

The useful working range of film-covered electrodes depends on the solvent and substrate. In MeCN the potential limits of film-covered electrodes were governed by the film electrochemistry. At negative potentials (< -0.3 V) the film became insulating whereas large positive potentials resulted in the loss of film oxidation and reduction. In 0.1N H₂SO₄ the limits were caused by proton reduction at negative potentials. These limits at PP-coated electrodes were nearly identical to those at the bare substrate. Films of thicknesses ranging from 0.06 to 1.14 μm on Pt showed a sharp cathodic current increase at -0.32 V as did bare Pt. Current densities at this potential increased with film thickness because of simultaneous reduction of PP. At Ta/PP proton reduction was observed at -1.1 to -1.2 V. Current densities were independent of film thickness up to 0.32 μm .

The anodic limits in 0.1N H₂SO₄ were similar to those in MeCN with a loss of film properties occurring upon film oxidation. Water oxidation could be observed at $\sim +1.4$ V at Pt/PP, similar to that on bare Pt. Continued gas evolution at those electrodes resulted in blistering of the film and a decrease in film activity.

Impedance measurements in supporting electrolytes.—Typical impedance vs. potential curves for a Pt electrode coated with 0.21 μm of PP are shown in Fig. 3. When the potential was scanned toward positive values from 0.1V vs. SCE, both capacitance and conductance increased with potential, corresponding to the oxidation of the PP film observed in the cyclic voltammogram. At the potential ($\sim +0.8$ V vs. SCE), where an anodic peak is observed in the cyclic voltammograms, the ad-

Table I. Cyclic voltammetric scan rate dependence of Pt/PP in 0.2M TBABF₄-MeCN in background current region

ν (V/sec)	i_a/ν (mA/sec/V)	i_c/ν	$i_a/\nu^{1/2}$ (mA sec ^{1/2} /V ^{1/2})	$i_c/\nu^{1/2}$
A. 0.19 μm film				
0.010	36.4	3.18	3.64	3.18
0.020	36.4	2.95	5.14	4.18
0.050	30.5	2.45	6.81	5.45
0.100	20.9	1.77	6.61	5.60
0.200	13.0	1.02	5.79	4.57
0.500	9.1	0.72	6.43	5.14
B. 1.0 μm film				
0.010	10.71	8.57	1.07	0.86
0.020	9.65	8.04	1.36	1.14
0.050	7.86	6.43	1.76	1.44
0.100	6.77	4.36	2.15	1.69
0.200	4.46	3.57	2.15	1.60
0.500	3.74	1.64	2.22	1.16

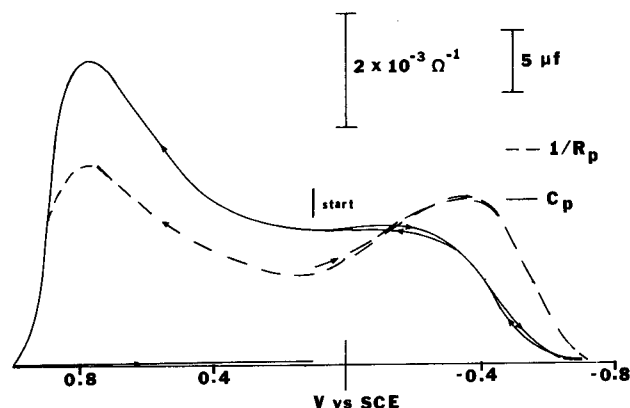


Fig. 3. $1/R_p$ and C_p vs. potential for $0.074 \mu\text{m}$ PP on Pt in 1M KCl. $\omega = 100 \text{ Hz}$, $v = 5 \text{ mV/sec}$.

mittance decreased sharply to a very small value. The admittance previously found at less positive potentials could not be restored in subsequent cathodic and anodic scans, suggesting that the film had permanently lost its electrochemical activity as well as its conductivity. The admittance of the PP film was much more stable if the potential was not scanned beyond $+0.6\text{V vs. SCE}$. When the potential was scanned toward negative potentials from $+0.1\text{V}$, the admittance showed a broad peak in the potential region where the redox behavior of the film is observed. Both the capacitance and conductance decreased to very small values when the potential became more negative than -0.7V . However, in this case, the admittance could be restored by a subsequent anodic scan, indicating the reversible behavior of the electrochemical activity of the film in this potential region. This loss of the admittance confirms the insulating nature of the reduced film.

In the remainder of this section, we discuss results only in the potential region around $+0.1\text{V vs. SCE}$, where negligible faradaic processes occur. In this region, the admittance can primarily be attributed to double layer charging. Some prominent features of the double layer charging admittance are:

1. As shown in Fig. 4, the parallel capacitance, C_p , and the parallel conductance, $1/R_p$, of Pt/PP in 1M KCl at 100 Hz are proportional to the film thickness. A similar linear dependence was also obtained with $0.5\text{M Na}_2\text{SO}_4$, 1M NaClO_4 , or 1M LiCl . Thus

$$C_p \propto l \quad [1]$$

$$1/R_p \propto l \quad [2]$$

2. The slope of the $1/R_p$ vs. film thickness, l , plot is higher than that of the C_p vs. l plot by a factor of ω , the angular frequency of the small a-c excitation.

3. Extremely large capacitances and conductances are observed on Pt/PP electrodes. For film thickness of $0.10 \mu\text{m}$, the C_p and R_p values of a polymer-coated Pt electrode in 1M KCl at 100 Hz are 30-50 times higher than those of a bare Pt electrode.

4. The capacitances and conductances of Pt/PP are strongly dependent on the supporting electrolytes, e.g., $1/R_p$ and C_p in 1M KCl are 5-10 times higher than those in $0.5\text{M Na}_2\text{SO}_4$, although on bare Pt, the capacitance and the conductance are nearly the same for these two solutions.

5. As shown in Fig. 5, when ω is much less than a characteristic value, ω_0 , (e.g., 600 sec^{-1} in this case), C_p is essentially independent of ω while $1/R_p$ is linearly proportional to ω . When ω is much greater than ω_0 , $1/R_p$ is proportional to $\omega^{1/2}$ and C_p is inversely proportional to $\omega^{1/2}$. Thus

$$1/R_p \propto \omega \quad (\omega \ll \omega_0) \quad [3]$$

and

$$C_p \propto \omega^{-1/2} \quad [4]$$

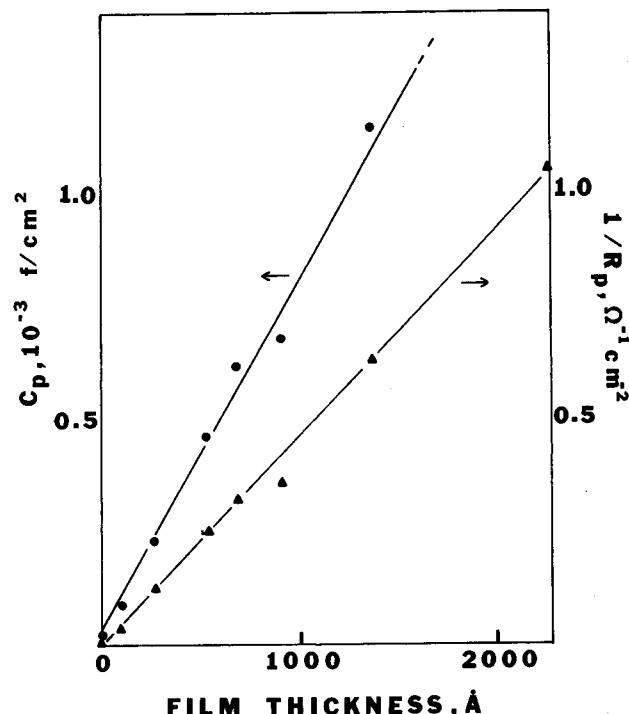


Fig. 4. The dependence of parallel capacitance and conductance on film thickness for PP on Pt in 1M KCl. $\omega = 100 \text{ Hz}$, $v = 5 \text{ mV/sec}$.

$$1/R_p \propto \omega^{1/2} \quad (\omega \gg \omega_0) \quad [5]$$

In $0.5\text{M Na}_2\text{SO}_4$, the frequency dependency of C_p and $1/R_p$ essentially follows Eq. [4] and [5] in the frequency range studied (2-2 kHz).

Electrochemistry of solution redox species.—The oxidation of 1 mM ferrocene (Cp_2Fe) at Pt/PP in $0.2\text{M TBABF}_4\text{-MeCN}$ yielded cyclic voltammograms very similar to those observed at a bare Pt electrode, as previously reported (5). The separation of the peak potentials, ΔE_p , was $\sim 70 \text{ mV}$ for scan rates up to 100 mV/sec ; the E_p values were constant with $(E_{pa} + E_{pc})/2 = +0.41\text{V}$. Peak currents at film-covered electrodes ($0.1\text{-}0.3 \mu\text{m}$) were slightly smaller than those at the bare Pt.

At Ta/PP, well-defined waves were observed (Fig. 6). Data are presented in Table II for a $0.32 \mu\text{m}$ film in 1.61 mM FeCp_2 . The ΔE_p values were larger than at Pt/PP, 80 mV at low scan rates to 200 mV at scan rates above 100 mV/sec . These films were somewhat less stable to cycling than films on Pt, with currents slowly decreasing. As in the absence of Cp_2Fe , the decay was accelerated by scanning to potentials more positive than $+0.6\text{V}$. At a polished Ta electrode in the same solution, little well-defined electrochemistry was observed. Overall currents were less than 20% of those at Ta/PP.

In $7.8 \text{ mM Fe(CN)}_6^{4-}$ in $0.1\text{N H}_2\text{SO}_4$, Pt/PP yielded well-defined cyclic voltammetric waves. Data in Table III are for two film thicknesses. The ΔE_p 's were $75\text{-}100 \text{ mV}$ at scan rates up to 500 mV/sec for films up to $0.4 \mu\text{m}$ thick. Thicker films gave larger ΔE_p values, 90 mV at 10 mV/sec to 125 mV at 200 mV/sec . Peak currents and E_p values were similar to those at bare Pt and i_p varied linearly with $v^{1/2}$ up to 100 mV/sec .

At Ta/PP in the same electrolyte, well-defined redox waves were observed (Fig. 7). The ΔE_p 's were somewhat larger and current densities smaller than at Pt/PP, as seen in the data in Table III. Increasing film thickness up to $0.38 \mu\text{m}$ had little effect on the CV behavior. The stability of films on Ta was slightly lower

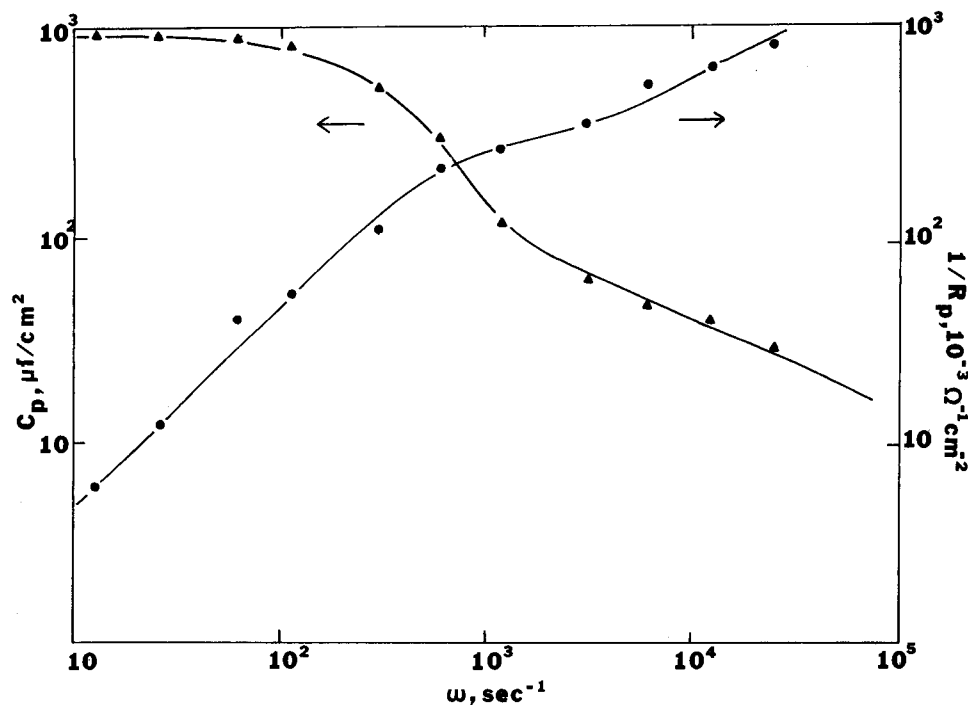


Fig. 5. Frequency dispersions of the parallel capacitance and conductance for 0.1 μm PP on Pt in 1M KCl. $v = 5$ mV/sec.

than on Pt. However, the decay of peak currents could be minimized by keeping the sweep limits between +0.1 and +0.6V. Scanning through the film redox waves resulted in a more rapid decay of $\text{Fe}(\text{CN})_6^{4-/3-}$ waves. Figure 7 also illustrates the CV of a bare polished Ta electrode in $\text{Fe}(\text{CN})_6^{4-}/0.1\text{N H}_2\text{SO}_4$.

A previous report from this laboratory discussed the application of a PP coating on an n-Si electrode covered with a thin gold film ($\sim 15\text{\AA}$) in an $\text{Fe}(3+/2+)$, 10.5M LiCl electrolyte as a means of stabilizing irradiated n-Si (7). To test the inherent stability of PP under these conditions, a Ta/PP electrode in 10.5M LiCl containing 50 mM FeCl_2 was cycled through both

the $\text{Fe}^{2+}/\text{Fe}^{3+}$ and film redox regions. The data for this solution compared to 0.1N H_2SO_4 , and with Pt/PP as well, are shown in Table IV. The ΔE_p 's for the Ta electrode were larger than for Pt, and current densities were smaller for similar film thicknesses. Peak currents for films on Ta exhibited a negative deviation from linearity with $v^{1/2}$.

Halide oxidation.—While PP films appeared to be stable during oxidation of some solution redox couples (e.g., Fe^{2+} to Fe^{3+} in 10.5M LiCl) they decomposed during halide oxidation. A CV scan in a solution containing 50 mM Fe^{2+} and 10.5M LiCl to potentials where Cl^- oxidation occurred induced a rapid decrease in the

Table II. Cyclic voltammetry of 1.61 mM Cp_2Fe at 0.32 μm PP/Ta in 0.2M TBABF₄-MeCN

v (V/sec)	E_{pa} (V vs. SCE)	E_{pc} (V vs. SCE)	ΔE_p (mV)	i_{pa} (mA/cm ²)	$i_{pa}/v^{1/2}$	i_{pc} (mA/cm ²)	$i_{pc}/v^{1/2}$
0.005	+0.440	+0.380	60	0.15	2.1	0.10	1.4
0.010	0.450	0.370	80	0.18	1.8	0.14	1.4
0.020	0.450	0.370	80	0.27	1.9	0.14	1.0
0.050	0.480	0.355	105	0.42	1.9	0.27	0.9
0.100	0.475	0.350	125	0.65	2.1	*	
0.200	0.490	0.340	150	0.88	2.0	*	

* Not measurable.

Table III. Cyclic voltammetry of $\text{Fe}(\text{CN})_6^{4-}$ in 7.8 mM $\text{K}_4\text{Fe}(\text{CN})_6/0.1\text{N H}_2\text{SO}_4$

v (V/sec)	E_{pa} (V vs. SCE)	E_{pc} (V vs. SCE)	ΔE_p (mV)	i_{pa} (mA/cm ²)	$i_{pa}/v^{1/2}$	i_{pc} (mA/cm ²)	$i_{pc}/v^{1/2}$
A. 0.38 μm PP on Pt							
0.010	+0.355	+0.280	75	0.57	5.7	0.55	5.5
0.020	0.355	0.280	75	0.73	5.1	0.71	5.0
0.050	0.360	0.280	80	1.09	4.9	1.05	4.7
0.100	0.365	0.275	90	1.68	5.3	1.50	4.7
0.200	0.370	0.270	100	2.27	5.1	2.36	5.3
B. 1.14 μm PP on Pt							
0.010	+0.370	+0.280	90	0.59	5.9	0.64	6.4
0.020	0.375	0.270	105	0.77	5.5	0.91	6.4
0.050	0.375	0.290	95	1.18	5.3	1.23	5.5
0.100	0.385	0.270	115	2.00	6.3	1.73	5.5
0.200	0.390	0.265	125	2.27	5.1	1.36	3.1
C. 0.13 μm PP on Ta							
0.020	+0.380	+0.265	115	0.45	3.2	0.48	3.4
0.050	0.385	0.250	135	0.64	2.8	0.70	3.1
0.100	0.395	0.245	150	0.85	2.7	0.88	2.8
0.200	0.405	0.235	175	1.03	2.3	1.09	2.4
0.500	0.425	0.210	215	1.15	1.6	1.49	2.1

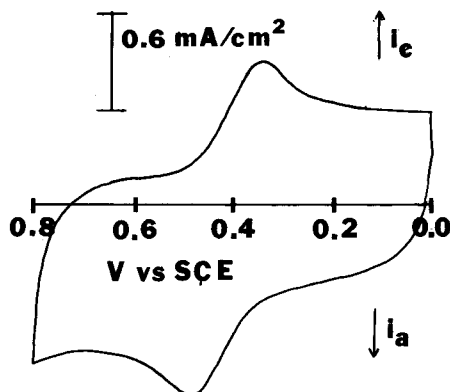


Fig. 6. Cyclic voltammogram of $0.30 \mu\text{m}$ PP on Ta in 1 mM $\text{Cp}_2\text{Fe-MeCN}$ (0.2M TBABF_4). $\nu = 100 \text{ mV/sec}$.

currents for both Cl^- and Fe^{2+} oxidation waves. In addition, little Cl_2 reduction was observed on reversing the potential sweep direction after Cl^- oxidation. Thus, PP appears to decompose upon evolution of Cl_2 . A similar instability exists during Br^- oxidation. For both Pt/PP and Ta/PP bromide oxidation commenced at $\sim +0.7\text{V vs. SCE}$ in saturated aqueous NaBr with Pt/PP. Scan reversal at $+0.8\text{V}$ resulted in a cathodic peak at $+0.57\text{V}$. The peak current for this wave was about 75% of that at bare Pt. However, after six scans between 0 and $+0.8\text{V}$, this peak current decreased to less than half of that of the initial scan. Continued scanning over the Br^- oxidation wave removed all film activity except for an increasing anodic current at potentials $> +0.7\text{V}$. After cycling in NaBr, no $\text{Fe}^{2+}/\text{Fe}^{3+}$ redox waves could be detected nor was any film oxidation or reduction observed.

Similar results were obtained for Ta/PP in saturated NaBr. In this case the cathodic peak of Br_2 reduction was broader at $+0.4\text{V}$. Continued scanning again resulted in diminished film activity. At a bare Ta electrode, only gradually increasing anodic currents were observed at potentials $> +1.0\text{V}$. No corresponding reduction wave was observed. Exposure of a PP film to an aqueous Br_2 solution for several hours resulted in a change in the film color from black to brown with loss of film electroactivity.

Discussion

The results of both the CV and impedance measurements demonstrate that the PP films are porous to solution species and solvent and that at least some of the electrochemical reaction can occur at the substrate material. This penetration of solvent and ions through the PP film was recently invoked to explain

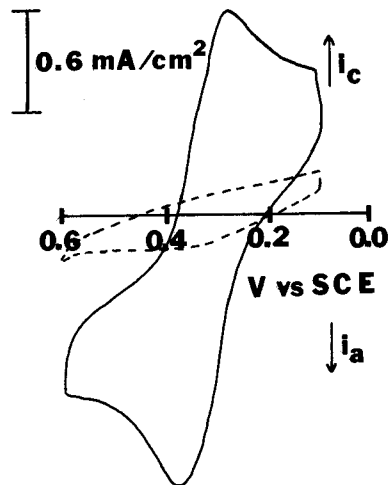


Fig. 7. Cyclic voltammogram of $0.13 \mu\text{m}$ PP on Ta (—) and bare polished Ta (---) in $7.8 \text{ mM Fe(CN)}_6^{4-}/-0.1\text{N H}_2\text{SO}_4$. $\nu = 100 \text{ mV/sec}$.

the slow decay of the photocurrent at an n-type silicon electrode coated with PP and the beneficial effect of the thin gold underlayer (7).

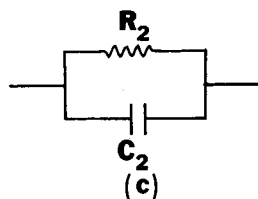
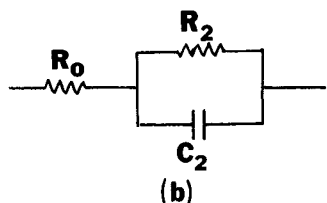
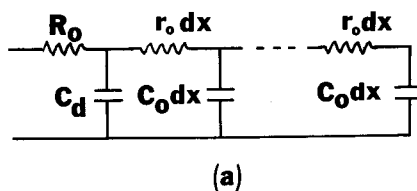
Consider first the impedance measurements in more detail. The impedance of porous electrodes has been discussed in detail in the literature based on the single-pore model (10). For simplicity, we assume that the PP films are composed of many essentially identical, noninterconnected channels. Each channel is assumed to have a uniformly distributed electrolyte and electrode resistance throughout its length. The resistance of the PP film is assumed to be negligibly small compared to the solution channel resistance. This is reasonable since the resistivity of the PP film (5) in the solid state is much smaller than the solution resistivity. With these assumptions, the PP film would be visualized as composed of numerous pores with their terminal ends connected to the bulk solution on one side and to the Pt surface or PP film on the other side. This procedure transforms the multipore problem into a single-pore problem. Based on the single-pore model and without considering the diffusion of supporting electrolyte inside the pore, the equivalent circuit of such a system is represented in Scheme Ia, where R_0 is the resistance of the bulk electrolyte, C_0 is the double layer capacitance per unit length of the pore, C_d is the double layer capacitance of the exposed substrate, r_0 is the resistance per unit length of the electrolyte channel, and dx is an infinitesimally small section of the pore. From circuit theory, Scheme Ia can be

Table IV. Cyclic voltammetry of Fe^{2+} at PP coated electrodes*

A. $0.26 \mu\text{m}$ PP on Pt							
ν (V/sec)	E_{pa} (V vs. SCE)	E_{pc} (V vs. SCE)	ΔE_p (mV)	i_{pa} (mA/cm^2)	$i_{pa}/\nu^{1/2}$	i_{pc} (mA/cm^2)	$i_{pc}/\nu^{1/2}$
0.010	+0.450	+0.380	70	0.96	9.6	0.92	9.2
0.020	0.455	0.385	70	1.29	9.1	1.23	8.7
0.050	0.460	0.360	100	1.82	8.1	1.77	7.9
0.100	0.470	0.355	125	2.46	7.8	2.31	7.3
0.200	0.480	0.350	130	3.54	7.9	2.94	6.6
0.500	0.500	0.330	170	5.77	8.2	3.85	5.4
B. $0.26 \mu\text{m}$ PP on Ta							
0.005	+0.470	+0.360	110	0.63	8.9	0.61	8.6
0.010	0.470	0.355	115	0.85	8.5	0.82	8.2
0.020	0.476	0.355	120	1.12	7.9	1.03	7.3
0.050	0.485	0.350	135	1.55	6.9	1.52	6.8
0.100	0.490	0.345	145	1.92	6.1	1.82	5.8
0.200	0.495	0.325	170	2.27	5.1	2.12	4.7
0.500	0.520	0.300	220	2.27	3.2	†	4.7

* The solution contained 50 mM FeCl_2 in 10.5M LiCl .

† Not measurable.



Scheme 1

further transformed into Scheme Ib, where R_2 and C_2 can be represented by the following equations for two extreme conditions (10b) when $\omega \gg \omega_0 = 2/l^2 C_0 r_0$, in which l is the solution penetration depth

$$R_2 = (2r_0/\omega C_0)^{1/2} \quad [6]$$

$$C_2 = C_d + (C_0/2r_0\omega)^{1/2} \quad [7]$$

When $\omega \ll \omega_0$

$$R_2 = 1/\omega C_0 l \quad [8]$$

$$C_2 = C_d + C_0 l \quad [9]$$

If $(1/1 + \omega^2 R_2^2 C_2^2) R_2 \gg R_0$, Scheme Ib can be simplified to Scheme Ic. Thus, R_2 is proportional to the parallel resistance, R_p , and C_2 is given by the parallel capacitance, C_p , and the average number of channels in the film.

Comparing Eq. [1]-[5] with Eq. [6]-[9], one sees that the experimental results fit this model quite well, even though the PP film may be very inhomogeneous microscopically and the actual channel arrangement deviates from that assumed in the single-pore model calculations. The characteristic angular frequency, ω_0 is strongly dependent on the solution penetration depth, the resistance, and capacitance per unit length of the pore.

In the derivation of Eq. [6]-[9], mass transfer effects have been neglected. However, this neglect might be invalid if electrolyte ions are sufficiently big that their mass transport rate is slowed and their concentration decreased inside the channel. In general, the impedance measurements are consistent with a porous electrode which becomes insulating, irreversibly, at scans beyond $\sim +0.8V$ and reversibly at scans beyond $\sim -0.4V$.

The question we have also attempted to answer is whether or not these films are porous enough to allow small electroactive species to undergo electron transfer at the substrate surface rather than at the PP surface. Some evidence for this is seen in the potentials for H^+ reduction in 0.1N H_2SO_4 . If reduction occurred at the film surface, one would not expect the potential to be a function of the substrate. Gas production at the substrate/film interface is the most probable cause of the observed blistering of the film. This caused a loss

of film activity, but no visible loss of film from the electrode. In extreme cases, thicker films could be removed from the electrode surface intact after gas evolution.

The apparent instability of PP films on Ta in 0.1N H_2SO_4 is very likely not due to decomposition of the film itself. The diffusion of solvent through the film possibly causes oxidation of the Ta, gradually undermining the PP film so that its electrochemistry is no longer observed. This behavior was not observed for PP on Pt, and the film could still be seen on the electrode, even when there was very little film activity. The better stability with 10.5M LiCl also implies substrate reaction with solvent. Polypyrrole films are unstable to oxidative conditions. The irreversible oxidation observed at +1.0V in aqueous media is likely due to the formation of an oxypyrrole polymer which has been shown to have lower conductivity than the polymer formed in MeCN (5d). Chemical instability to halogens is not surprising, since PP's in general react with halogens. As the CV data in Cl^- and Br^- media demonstrate, the oxidation of the halide ions occurs readily and the resulting electrogenerated halogens gradually attack the polymer, leading to the decreasing Br_2 reduction waves in successive scans.

Although PP films appear to be porous to solvent and electrolyte, electron transfer reactions can occur at the PP surface itself. Redox waves can be observed at Ta/PP that are not observed at bare Ta. These CV waves appear less reversible than those at bare Pt or Pt/PP, but they are well defined.

The cyclic voltammetric response is independent of film thickness for thin films on both Pt and Ta. This suggests an electronic conduction mechanism. However, there is still some ionic diffusion, as seen in the less reversible behavior at thick PP films on Pt.

Acknowledgments

The support of Texas Instruments and the Solar Energy Research Institute is gratefully appreciated. Also, we would like to thank Dr. Rommel Noufi for his helpful discussions concerning this work.

Manuscript submitted Aug. 21, 1981; revised manuscript received Nov. 24, 1981.

Any discussion of this paper will appear in a Discussion Section to be published in the December 1982 JOURNAL. All discussions for the December 1982 Discussion Section should be submitted by Aug. 1, 1982.

Publication costs of this article were assisted by The University of Texas.

REFERENCES

- (a) R. D. Rocklin and R. W. Murray, *J. Phys. Chem.*, **85**, 2104 (1981); (b) N. Oyama and F. C. Anson, *Anal. Chem.*, **52**, 1192 (1980); (c) P. J. Pearce and A. J. Bard, *J. Electroanal. Chem. Interfacial Electrochem.*, **112**, 97 (1980).
- M. S. Wrighton, R. G. Austin, A. B. Bocarsly, J. M. Bolts, O. Haas, K. D. Legg, L. Nadjo, and M. C. Palazzotto, *J. Am. Chem. Soc.*, **100**, 1602 (1978).
- P. J. Pearce and A. J. Bard, *J. Electroanal. Chem. Interfacial Electrochem.*, **108**, 121 (1980).
- A. Dall'Olio, G. Dascola, V. Varacca, and V. Bocchi, *Comp. Rend.*, **433**, 267c (1968).
- (a) A. F. Diaz and K. K. Kanazawa, *J. Chem. Soc., Chem. Commun.*, 635 (1979); (b) K. K. Kanazawa, A. F. Diaz, R. H. Geiss, W. D. Gill, J. F. Kwak, J. A. Logan, J. F. Rabolt, and G. B. Street, *ibid.*, 854 (1979); (c) A. F. Diaz and J. I. Castillo, *ibid.*, 397 (1980); (d) K. K. Kanazawa, A. F. Diaz, W. D. Gill, P. M. Grant, G. B. Street, and G. P. Gardini, *Synthetic Metals*, **1**, 329 (1979/1980); (e) A. Diaz, J. M. Vasquez Vallejo, and A. Martinez Duran, *IBM J. Res. Develop.*, **25**, 42 (1981).
- (a) R. Noufi, A. J. Frank, and A. J. Nozik, *J. Am. Chem. Soc.*, **103**, 1849 (1981); (b) R. Noufi, D. Tench, and L. F. Warren, *This Journal*, **127**, 2310 (1980); (c) T. Skotheim, I. Lundström, and J. Prejza, *This Journal*, **128**, 1625 (1981).

7. F.-R. F. Fan, B. Wheeler, A. J. Bard, and R. Noufi, *ibid.*, **128**, 2042 (1981).
8. P. J. Peerce and A. J. Bard, *J. Electroanal. Chem. Interfacial Electrochem.*, **112**, 97 (1980).
9. "Encyclopedia of Electrochemistry of the Elements," Vol. 2, A. J. Bard, Editor, Marcel Dekker, Inc., New York (1974).
10. (a) R. DeLevie, in "Advances in Electrochemistry and Electrochemical Engineering," Vol. 6, P. Delahay, Editor, Interscience, New York (1967); (b) D. I. Leikis, E. S. Sevast'yanov, and L. L. Knots, *Russ. J. Phys. Chem.*, **38**, 997 (1964).
11. F.-R. F. Fan and A. J. Bard, *This Journal*, **128**, 945 (1981).

